Impurity Capacities of Non-ferrous Slags

R. G. Reddy

Professor, The University of Alabama, Tuscaloosa, Alabama, USA 35487;
Email: rreddy@eng.ua.edu

Keywords: Slags, Reddy-Blander model, Non-ferrous metals, Impurity Capacities

ABSTRACT

The complexity in treating environmentally harmful impurities such as As, Sb, Bi from the base metal matte or metal in the smelting stage are responsible for the high cost of the refining process. The impurity capacities (such as arsenic, antimony and bismuth) of slags were calculated *a priori* using Reddy-Blander (RB) model. The capacity predictions were for a wide range of matte and slag compositions in copper smelting conditions. The calculated impurities capacities and impurity distribution ratios results are in good agreement with the available experimental and industrial slags data. The *a priori* knowledge of impurities is useful for reduction of energy consumption and enhanced environmental control in the current and future non-ferrous metal processes.

INTRODUCTION

Impurity capacity of a slag is defined as a measure of the ability of slag to hold the impurity. The common minerals that contain As, Sb and Bi in copper are Arsenopyrite (FeAsS), Enargite (Cu_3AsS_4), Lautite (CuAsS), Tennantite [$(Cu,Fe)_{12}As_4S_{13}$], Famatinite (Cu_3SbS_4), Chalcostibite ($CuSbS_2$), Wittichenite (Cu_3BiS_3), Emplectite ($CuBiS_2$), and Aikinite ($PbCuBiS_3$). The lead impurity compounds are Jordanite ($Pb_{14}As_6S_{23}$), and Cosalite (Pb_2Bi_2S) (Larouche,2001).

In copper, nickel and lead sulfide smelting and refining, removal of sulfur, arsenic, antimony, and bismuth cause metal losses in both entrained and chemically dissolved forms in the slags. As a result, an understanding of impurity capacity of slags is essential for the development of clean metal technology. The Reddy-Blander (RB) model, first proposed in 1987 (Reddy and Blander, 1987), predicted that sulfide capacities can be calculated *a prior* based on a simple solution model and on the knowledge of chemical and solution properties of sulfides and oxides.

The sulfide capacities of several binary silicate (Reddy and Blander, 1987; Reddy and Blander, 1989; Reddy et al., 1992, Reddy, 2003), aluminate (Reddy and Zhao, 1995), titanate (Derin et al., 2004), multi-component silicate (Yahya and Reddy, 2011; Chen et al., 1989; Pelton et al., 1993; Bora et al., 2011) and industrial slags (Derin and Reddy, 2003; Derin et al., 2005, 2006) were predicted using the RB model. The model was also applied for sulfate (Pelton, 1999), arsenate (Reddy and Font, 2003), antimonate, Font and Reddy, 2005) capacities in slags and sulfur and oxygen partial pressures in copper slags (Derin and Reddy, 2003). brief description of the RB model is presented on the thermodynamic modeling of impurity capacity section. Impurity capacity expressions for several impurities are presented in Table 1. (Reddy, 2003a).

TABLE 1-Capacities expression for different species.

Species, i	Reaction	Capacity, C_i
Sulfide, $[S^{2-}]$	$\frac{1}{2}S_2(g) + [O^{2-}] = [S^{2-}] + \frac{1}{2}O_2(g)$	$C_S = (wt\%S)\left(\frac{P_{O_2}}{P_{S_2}}\right)^{\frac{1}{2}}$
Pyrosulfate, $[S_2O_7^{2-}]$	$S_2(g) + [O^{2-}] + 3O_2(g) = [S_2O_7^{2-}]$	$C_{S_2O_7^{2-}} = \frac{\left(wt\%S_2O_7^{2-}\right)}{P_{O_2}^3 P_{S_2}}$
Sulfate, $[SO_4^{2-}]$	$\frac{1}{2}S_2(g) + [O^{2-}] + 3/2O_2(g) = [SO_4^{2-}]$	$C_{SO_4^{2-}} = \frac{(wt\%SO_4^{2-})}{P_{O_2}^{\frac{3}{2}} P_{S_2}^{\frac{1}{2}}}$
Carbide, $[C_2]$	$3C(gr) + [O^{2-}] = [C_2^{2-}] + CO(g)$	$C_{C_2} = wt\%C_2 \frac{P_{CO}}{a_C^3}$
Carbonate, $[CO_3^{2-}]$	$CO_2(g) + [O^{2-}] = [CO_3^{2-}]$	$C_{CO_3^{2-}} = \frac{\left(wt\%CO_3^{2-}\right)}{P_{CO_2}}$
Hydroxyl, $[OH^-]$	$1/2H_2O(g) + 1/2\,[O^{2-}] = [OH^-]$	$C_{OH^-} = \frac{\left(wt\%OH^-\right)}{P_{H_2O}^{\frac{1}{2}}}$

Nitride, $[N^{3-}]$	$1/2N_2(g) + 3/2[O^{2-}] = [N^{3-}] + 3/4O_2(g)$	$C_N = \left(wt\%N^{3-}\right)\frac{P_{O_2}^{\frac{3}{4}}}{P_{N_2}^{\frac{1}{2}}}$
Cyanide, $[CN^-]$	$N_2(g) + 3C + [O^{2-}] = 2[CN^-] + CO(g)$	$C_{CN^-} = \left(wt\%CN^-\right)\frac{P_{CO}^{\frac{1}{2}}}{a_C^{\frac{3}{2}}P_{N_2}^{\frac{1}{2}}}$
Phosphate, $[PO_4^{3-}]$	$P_2(g) + 3[O^{2-}] + 5/2O_2(g) = 2[PO_4^{3-}]$	$C_{PO_4^{3-}} = \frac{\left(wt\%PO_4^{3-}\right)}{P_{O_2}^{\frac{5}{4}}P_{P_2}^{\frac{1}{2}}}$
Phosphide, $[P^{3-}]$	$1/2P_2(g) + 3/2[O^{2-}] = [P^{3-}] + 3/4O_2(g)$	$C_{P^{3-}} = \left(wt\%P^{3-}\right)\frac{P_{O_2}^{\frac{3}{4}}}{P_{P_2}^{\frac{1}{2}}}$
Arsenate, $[AsO_4^{3-}]$	$3/2O^{2-} + As(l) + 5/4O_2(g) = AsO_4^{3-}$	$C_{AsO_4^{3-}} = \frac{\left(wt\%AsO_4^{3-}\right)}{a_{As}P_{O_2}^{\frac{5}{4}}}$
Bismuthate,$[BiO_4^{3-}]$	$3/2O^{2-} + Bi(l) + 5/4O_2(g) = BiO_4^{3-}$	$C_{BiO_4^{3-}} = \frac{\left(wt\%BiO_4^{3-}\right)}{a_{Bi}P_{O_2}^{\frac{5}{4}}}$
Antimonate, $[SbO_4^{3-}]$	$3/2O^{2-} + Sb(l) + 5/4O_2(g) = SbO_4^{3-}$	$C_{SbO_4^{3-}} = \frac{\left(wt\%SbO_4^{3-}\right)}{a_{Sb}P_{O_2}^{\frac{5}{4}}}$
Telluride, $[Te^{2-}]$	$½Te_2(g) + [O^{2-}] = [Te^{2-}] + ½O_2(g)$	$C_{Te} = \left(wt\%Te\right)\left(\frac{P_{O_2}}{P_{Te_2}}\right)^{\frac{1}{2}}$
Selenide, $[Se^{2-}]$	$½Se_2(g) + [O^{2-}] = [Se^{2-}] + ½O_2(g)$	$C_{Se} = \left(wt\%Se\right)\left(\frac{P_{O_2}}{P_{Se_2}}\right)^{\frac{1}{2}}$

THERMODYNAMIC MODELING OF IMPURITY CAPACITY

Reddy-Blander (RB) Model: Impurity Capacity:

The Reddy-Blander model was used to predict the arsenic capacity of slags, metal and mattes. The arsenic capacity model (a measure of the ability of an oxide system or slag to hold arsenic), that can *a priori* predict the arsenic behavior in copper mattes and slags was derived (Reddy and Font, 2003). For the MO-SiO_2 system, the arsenic equilibrium reaction can be written as:

$$\frac{3}{2}\mathrm{MO}(l) + \mathrm{As}(l) + \frac{5}{4}O_2(g) = M_{3/2}\mathrm{AsO}_4(l) \qquad 1$$

where, M is arsenate compound forming element (such as Fe, Ca, Mg, .). The most stable arsenic compound in copper smelting slags is $M_{3/2}AsO_4$. At high oxygen partial pressures, the arsenic dissolve into the slag as As_2O_5 (Kojo, et al, 1984). The equilibrium constant, K_M, for the above reaction is:

$$K_M = \frac{a_{M_{3/2}\mathrm{AsO}_4}}{a_{\mathrm{MO}}^{3/2}\, a_{\mathrm{As}}\, p_{O_2}^{5/4}} \qquad 2$$

The arsenic capacity, C_{As}, in terms of measurable quantities was defined by Reddy (2003a) as:

$$C_{\mathrm{AsO}_4^{3-}} = \frac{(\text{wt pct AsO}_4^{3-})}{a_{\mathrm{As}}\, p_{O_2}^{5/4}} \qquad 3$$

Combining equations 2 and 3, the equation 4 can be obtained.

$$C_{AsO_4^{3-}} = (\text{wt pct } AsO_4^-)\ \frac{K_M\ a_{MO}^{3/2}}{a_{M_{3/2}AsO_4}} \qquad 4$$

Development of this expression was made considering two compositions ranges.

A. Arsenic Capacity for Basic Melts (0 $\leq X_{SiO_2} \leq$ 0.33)

The arsenic capacity for the basic melt in the MO-SiO_2 binary system becomes:

$$C_{AsO_4^{3-}} = \frac{100\ K_M\ a_{MO}^{3/2}\ W_{AsO_4}\ (1\text{-}2\ X_{SiO_2})}{\gamma_{M_{3/2}AsO_4}\ [W_{MO} + X_{SiO_2}(W_{SiO_2} - W_{MO})]} \qquad 5$$

Using RB model, similar expressions for the sulfide capacity of ferrous and non-ferrous slags in the silicate and aluminates systems were derived (Reddy and Blander, 1987; Reddy and Blander, 1989; Reddy et al., 1992; Reddy, 2003; Reddy and Zhao, 1995; Derin et al., 2004; Yahya and Reddy, 2011; Chen et al., 1989; Pelton et al., 1993; Bora et al., 2011; Derin and Reddy, 2003; Derin et al., 2005', 2006). By using the thermodynamic data for the equilibrium constant K_M, $\gamma_{M_{3/2}AsO_4}$, a_{MO} in the MO-SiO_2 binary system, and W is molecular weight of compounds arsenic capacities were calculated for several binary arsenic systems and are discussed in the section B.

B. Arsenic Capacity for Acidic Melts (0.33 $< X_{SiO_2} <$ 1)

In this composition range, the arsenic is dissolved in the MO-SiO_2 binary acidic melt that contains polymeric species. It is also assumed that the AsO_4^{3-} ion and the SiO_4 units in the polymer are similar in size and forms a chain with no free O^{2-} ions. For dilute solutions, the volume fraction of As ions sites in solution can be expressed as

$$\varphi_{As} = \frac{n_{As}}{n_{Si}} \qquad 6$$

The $C_{AsO_4^{3-}}$ for acidic melts is expressed as

$$C_{AsO_4^{3-}} = \frac{100\ K_M\ a_{MO}^{3/2}\ X_{SiO_2} W_{AsO_4}}{[W_{MO} + X_{SiO_2}(W_{SiO_2} - W_{MO})]}\, e^{\left[\frac{1}{m} - 1 - \mu\right]} \qquad 7$$

where m is the average polymer chain length and μ is the interaction energy between the ions. The arsenic capacity of binary MO-SiO_2 system can be predicted using equations 5 and 7 for the entire composition range (0< X_{SiO_2} <1) and at a fixed temperature. As the composition crosses between the basic and acidic melts (at X_{SiO2} of 0.33), the transition in the arsenic capacity is predicted by equations 5 and 7 to a smooth and continuous.

For the FeO-SiO_2 binary system, the arsenate formation reaction can be written as:

$$\frac{3}{2}\mathrm{FeO}(l) + \mathrm{As}(l) + \frac{5}{4}O_2(g) = \mathrm{Fe_{3/2}AsO_4}(l), \quad \Delta G^\circ = -279.7\ \mathrm{kJ/mol\ at\ 1573\ K} \qquad 8$$

It is important to note that in calculating the ΔG° for equation 8, the values of ΔH° and ΔS° for As (l) and $Fe_{3/2}$ AsO_4(s) (Roine, 2022) were extrapolated from 1200 K and 811 K, respectively. The ΔG° for the liquid $Fe_{3/2}AsO_4$ (l) was estimated from the experimental arsenic solubility data at 1573K. The a_{FeO} in FeO-SiO2 binary system was calculated at 1573 K using FactSage software (Bale et al., 2002). The arsenic capacity, as predicted using equation 5, depends on temperature and activity coefficient of $Fe_{3/2}AsO_4$ (l). At a constant $\gamma_{Fe_{3/2}AsO_4}$, the arsenic capacity of FeO-SiO_2 melts decreases with an increase in temperature. Also, at a constant temperature, the arsenic capacity deceases with increase in $\gamma_{Fe_{3/2}AsO_4}$. The calculated arsenic capacities of melts using equations 5 and 7 at 1573K and $\gamma_{Fe_{3/2}AsO_4}$ equal to 1. The arsenic capacity increases with increase in FeO content and shows a strong dependence on the activity of FeO in the melt. The K_M is the equilibrium constant for the R (arsenate, antimonate and bismuthate) forming reaction. The values of K_M arsenates, antimonates and bismuthate at 1573 K are given in Table 2 (Font and Reddy, 2003).

$$\frac{3}{2}\mathrm{MO}\ (l) + \mathrm{R}\ (l) + \frac{5}{4}O_2\ (g) = M_{3/2}\mathrm{RO_4}\ (\mathrm{s, l}) \qquad 9$$

TABLE 2 - Equilibrium Constants for Impurity Forming Reactions at 1573 K

	Log K_M		
M*	**Arsenate**	**Antimonate**	**Bismuthate**
Fe**	11.0	10.4	9.6
Ca	10.3	NA	NA
Mg	10.2	9.6	NA
Cu	-4.7	-6.0	NA
Ni	3.4	3.1	NA

NA: Not Available. * Reference state: Solid. ** Reference state: Liquid

The arsenic capacities of $CaO\text{-}SiO_2$ and $MgO\text{-}SiO_2$ binary melts were calculated using equations 5 and 7. The arsenic reactions for $CaO\text{-}SiO_2$ and $MgO\text{-}SiO_2$ melts are as follows:

$$\frac{3}{2}\mathrm{CaO}(l) + \mathrm{As}(l) + \frac{5}{4}O_2(g) = \mathrm{Ca_{3/2}AsO_4}(s), \quad \Delta\mathrm{G}^\circ = -362.50\ \mathrm{KJ/mol\ \ at\ 1573K} \qquad 10$$

$$\frac{3}{2}\mathrm{MgO}(l) + \mathrm{As}(l) + \frac{5}{4}O_2(g) = \mathrm{Mg_{3/2}AsO_4}(s), \quad \Delta\mathrm{G}^\circ = -338.14\ \mathrm{KJ/mol\ \ at\ 1573\ K} \qquad 11$$

The ΔG° for the reaction of $\mathrm{Ca_{3/2}AsO_4}(s)$ in equation 10 is taken from the reported data (Bale et al., 2002), and the ΔG° for equation 11, the values of ΔH° and ΔS° for As(l) and $Mg_{3/2}AsO_4$(s) (Roine, 2022) were extrapolated from 1200 K and 1225 K, respectively. The activities of CaO and MgO in melts at 1573 K were calculated (Bale, et. al., 2002). The arsenic capacity in the hypothetical melts of $CaO\text{-}SiO_2$ and $MgO\text{-}SiO_2$ binary systems were calculated. In the $CaO\text{-}SiO_2$ system, a sharp increase in arsenic capacity above the X_{CaO} value of 0.6 was observed (Reddy and Font, 2003). At higher compositions X_{CaO} equal to 0.8 and greater, no significant changes in arsenic capacities were observed. This is mainly due to the variation in the activity of CaO, a_{CaO} in the $CaO\text{-}SiO_2$ binary melts, which shows a strong negative deviation. Similar observations were made for $MgO\text{-}SiO_2$ melts. But the decrease in arsenic capacity in $MgO\text{-}SiO_2$ melts with an increase in the concentration of SiO_2 is much smaller than in the $CaO\text{-}SiO_2$ melts.

C. Arsenic Capacity in the Multi-component Systems

For multi-component system which contains only one acidic component such as SiO_2 (e.g., $FeO\text{-}CaO\text{-}SiO_2$ ternary system or FeO-CaO-MgO-SiO2 quaternary system), the arsenate formation reactions for CaO-, and FeO- can be expressed as;

$$\frac{3}{2}(\mathrm{FeO, CaO})(l) + \mathrm{As}(l) + \frac{5}{4}O_2(g) = (\mathrm{Fe, Ca})_{3/2}\mathrm{AsO_4}(l) \qquad 12$$

Using the Flood-Grjotheim approximation (Chen et al., 1989, Flood and Grjotheim, 1952), the partial Gibbs energies of mixing for different oxidative species are comparably similar. Thus, for a ternary system, the standard Gibbs energy change of mixing is expressed as

$$\Delta G_{(Fe,Ca)O} = N_{\mathrm{FeO}}\Delta G_{\mathrm{FeO}} + N_{\mathrm{CaO}}\Delta G_{\mathrm{CaO}} \qquad 13$$

where $\Delta G_{(\mathrm{Fe,\ Ca})O}$, ΔG_{FeO} and ΔG_{CaO} are the Gibbs energy changes for equations 12, 8 and 10, respectively. The N_{FeO} and N_{CaO} are the electrical equivalent cationic fractions ($N_{\mathrm{FeO}} = \frac{X_{\mathrm{FeO}}}{X_{\mathrm{FeO}}+X_{\mathrm{CaO}}}$ and $N_{\mathrm{CaO}} = \frac{X_{\mathrm{CaO}}}{X_{\mathrm{FeO}}+X_{\mathrm{CaO}}}$), and by considering the definition of Gibbs energy (ΔG = - RT ln K), equation 13 is further simplified as;

$$\log \mathrm{K}_8 = N_{\mathrm{FeO}} \log \mathrm{K}_5 + N_{\mathrm{CaO}} \log \mathrm{K}_6 \qquad 14$$

where K_8, K_5, and K_6 are the equilibrium constant for equations 12, 8 and 10 respectively. For a constant X_{SiO_2} in the $FeO\text{-}SiO_2$ and $CaO\text{-}SiO_2$ binary systems, the arsenic capacity is expressed as $C'_{\mathrm{AsO_4^{3-}(FeO)}} = K_{\mathrm{FeO}}\, a_{\mathrm{FeO}}^{3/2}$ and $\mathrm{C}'_{\mathrm{AsO_4^{3-}(CaO)}} = K_{\mathrm{CaO}}\, a_{\mathrm{CaO}}^{3/2}$. Thus, after substituting in equation 14 and rearranging , equation 15 is obtained.

$$\log C'_{AsO_4^{3-},(Fe,Ca)O} - \frac{3}{2}\log a_{(Fe,Ca)O} = N_{FeO}\left(\log C'_{AsO_4^{3-},FeO} - \frac{3}{2}\log a_{FeO}\right) + N_{CaO}\left(\log C'_{AsO_4^{3-},CaO} - \frac{3}{2}\log a_{CaO}\right) \quad 15$$

Furthermore, taking into consideration only (Fe, Ca)O as a solution, then the integral Gibbs energy of solution for equation 13 becomes $\log a_{(Fe,Ca)O} = N_{FeO}\log a_{FeO} + N_{CaO}\log a_{CaO}$. After substituting in equation 15 and rearranging it, the arsenic capacity for multi-component system is expressed as

$$\log C_{AsO_4^{3-},(Fe,Ca)O} = N_{FeO}\log C_{AsO_4^{3-},FeO} + N_{CaO}\log C_{AsO_4^{3-},CaO} \quad 16$$

The arsenic capacity of multi-component system using equation 16 can be calculated at a constant composition of acidic component (i.e. $X_{SiO2} + X_{FeO1.5}$) and is further discussed in the following section.

Evaluation of the Arsenic Capacity model

The phase equilibrium studies for arsenic between the FeO-MgO-SiO_2, FeO-CaO-MgO-SiO_2 slags and copper mattes at 1573K were reported (Roghani et al., 2000). The arsenic experimental data were reported in the form of distribution coefficients and solubility of arsenic in the slag. In the present study, an expression was derived between the distribution coefficient and arsenic capacity of slags in equilibrium with copper mattes.

Expression between Distribution Coefficient (L_{As}) and Arsenic Capacity (C_{AsO4}^{3-}):

The arsenic distribution coefficient between slag and matte phases is defined as

$$L_{As} = \frac{(\text{wt pct As in slag-oxidic phase})}{\{\text{wt pct As in matte - metal phase}\}} \quad 17$$

The weight pct of As in matte is expressed as

$$\{\text{Weight pct of As in matte}\} = \frac{a_{As(l)}\, W_{As}\{n_T\}}{\gamma_{As}} \quad 18$$

where $a_{As(l)}$ is activity of arsenic in matte, γ_{As} is activity coefficient of As in matte and W_{As} is the molecular weight of As, and $\{n_T\}$ is the total number of moles of matte phase. Combining equations 17, 18 and 3, after making the conversion of weight pct of As in slag, and rearranging, the relationship between the arsenic capacity and the L_{As} is obtained as

$$C_{AsO_4^{3-}} = \frac{L_{As}\, W_{AsO_4}\{n_T\}}{\gamma_{As}\, p_{O_2}^{5/4}} \quad 19$$

The experimental arsenic capacities were derived using equation 19 for each of the experimental L_{As} at 1573 K. The reported data of γ_{As} and p_{O_2} for Cu matte, were also used in the calculations.

Arsenic Capacity and Distribution Ratios between Cu mattes and Slags:

The RB model calculated *a priori* and experimental data for arsenic capacity and distribution ratios for FeO-$FeO_{1.5}$-$CuO_{0.5}$-MgO-SiO_2 slags and Cu mattes at 1573K are shown in Fig 1 and 2 respectively. The equilibrium constants for impurities reactions are presented in Table 2. The *a priori* predictions were calculated considering the reported data of γ_{As} for Cu matte, the a_{MO} for the MO-$FeO_{1.5}$-SiO_2 system, and the experimental pO_2 and $\{n_T\}$. A good agreement between the experimental data and RB model *a priori* calculated arsenic capacity and distribution ratio.

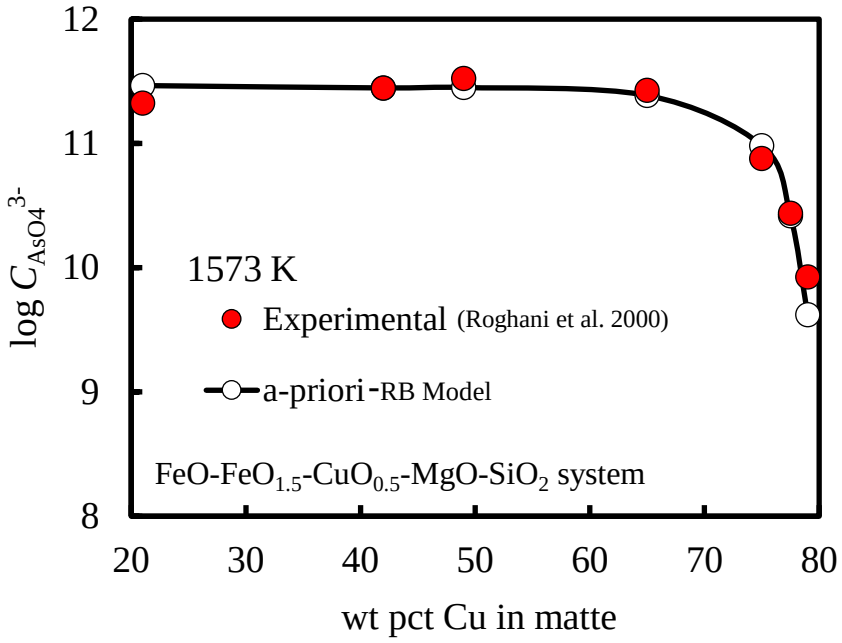

FIG 1-. Arsenic capacity of FeO-$FeO_{1.5}$-$CuO_{0.5}$-MgO-SiO_2 slag versus wt pct Cu in matte at 1573 K.

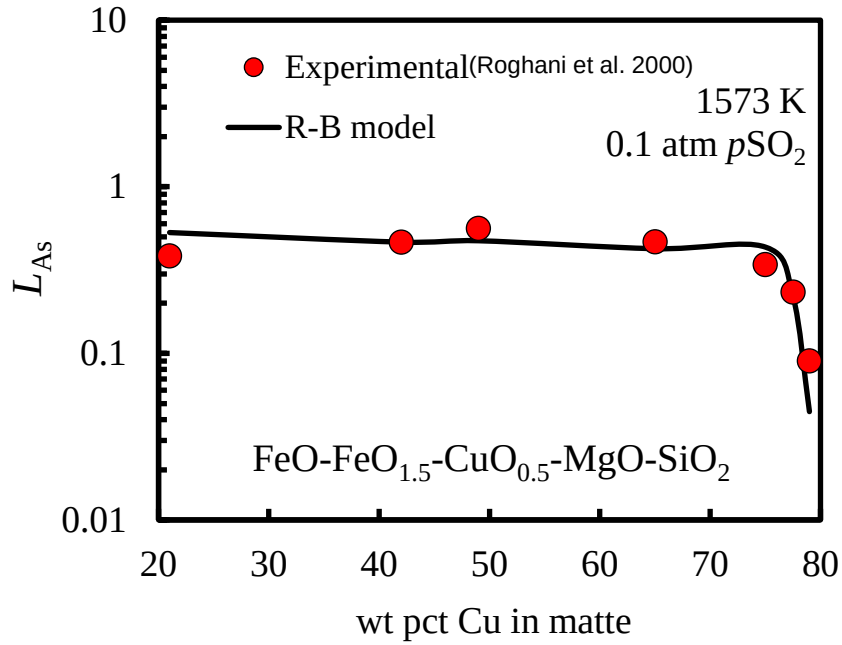

FIG 2- Distribution coefficient of arsenic of FeO-$FeO_{1.5}$-$CuO_{0.5}$-MgO-SiO_2 slag versus wt pct Cu in matte at 1573 K.

The slight deviations between the experimental and the calculated arsenic capacity may be due to the corresponding uncertainties of the experimental L_{As}, and the γ_{As} and p_{O_2} values (Roghani et al., 2000, Rosenqvist, 1983, Nikolov, et al., 1992, Roghani et al., 1997) used in equation 19 for deriving the experimental arsenic capacity. For the RB model arsenic capacity calculations using equation 16, the MgO content in the multi-component system was estimated by using the data of the FeO-$FeO_{1.5}$-$CuO_{0.5}$-MgO-SiO_2 system (Font et al., 1999, 1998, 1998a, 2000). Due to a lack of availability of thermodynamic data on liquid arsenates, the solid $Ca_{3/2}AsO_4$ and $Mg_{3/2}AsO_4$ data were used in calculating the Gibbs energy of the equation 10 and 11. Use of liquids data for these compounds will lower the arsenic capacity of these systems. The availability of reliable thermodynamic data for impurities in slags and mattes is essential. Further studies are in progress for extending this model

in *a priori* prediction of other impurities capacities such as Bi, Sb in copper matte and other non-ferrous metal smelting slags.

Antimonate Capacity and Distribution Ratio between Cu mattes and Slags:

The antimonate capacities were calculated using RB model for each of the slag composition and corresponding distribution ratios of Cu matte in equilibrium with the FeO-$FeO_{1.5}$- $CuO_{0.5}$ - MgO-SiO_2 slag at 1573 K and pSO_2 of 0.1 atm, using expressions similar to equations 5, 7 and 16. The antimony dissolved into the slag as Sb_2O_5 (Kojo, et al, 1984). The equilibrium constants for impurities reactions are presented in Table 2. The calculated using RB model for antimonate capacities and distribution ratios are shown in Fig 3 and 4 respectively. The data of γ_{Sb} for the Cu matte, the a_{MO} in the MO-SiO_2 binary system, and the experimental pO_2 and $\{n_T\}$ were used in the calculations. The *a priori* predictions and experimental data for antimony capacities and distribution ratios in slags and Cu mattes are in good agreement. The observed good agreement may be due to the including copper oxide data in slag system. This is particularly important at higher matte grades because higher solubility of copper into slags is reported (Roghani, et al., 2000).

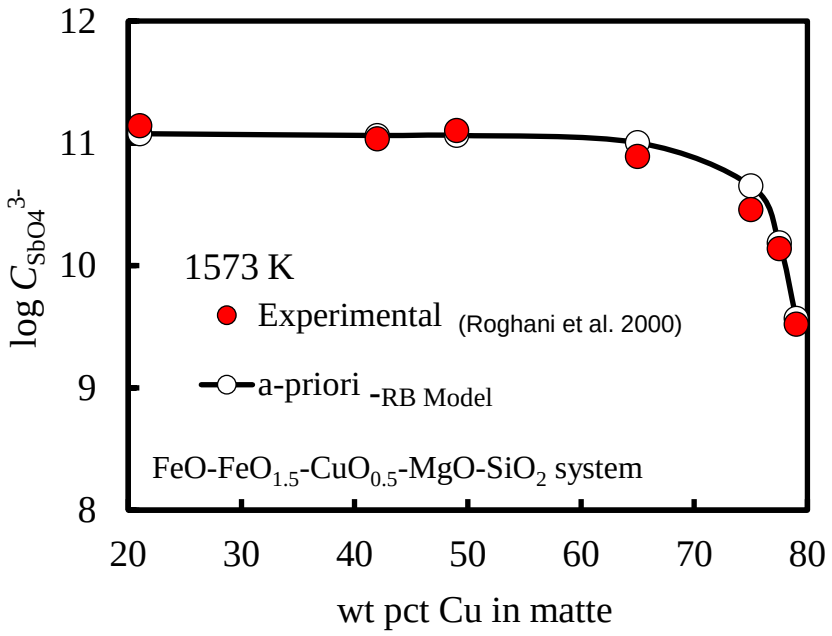

FIG 3-: Antimony capacity of FeO-$FeO_{1.5}$-$CuO_{0.5}$-MgO-SiO_2 slag vs wt pct Cu in matte at 1573 K.

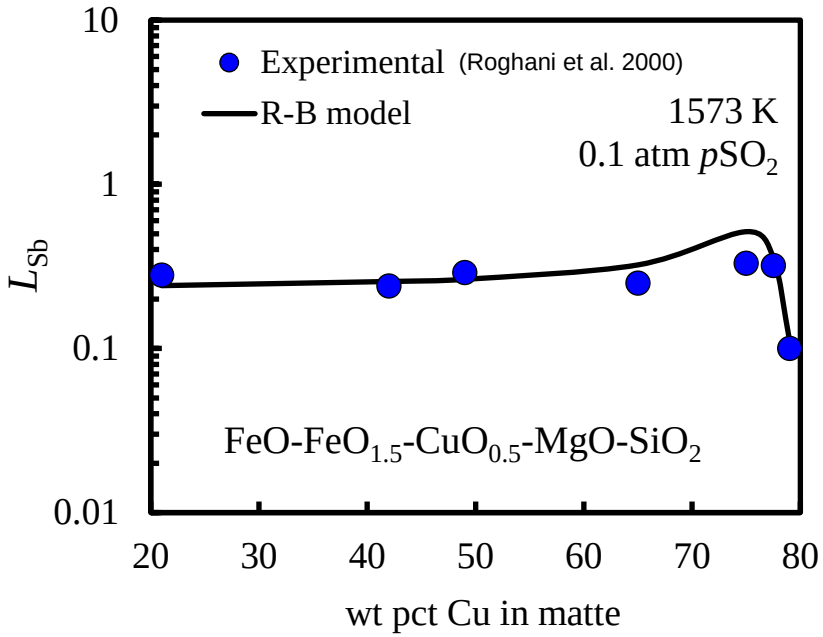

FIG 4- Distribution coefficient of antimony of $FeO\text{-}FeO_{1.5}\text{-}CuO_{0.5}\text{-}MgO\text{-}SiO_2$ slag vs wt pct Cu in matte at 1573 K

Bismuth Capacity and Distribution Ratios between Cu Mattes and Slags:

The bismuthate capacities and distribution ratios for Cu matte in equilibrium with the $FeO\text{-}FeO_{1.5}\text{-}SiO_2$ slag at 1573 K and pSO_2 of 0.1 atm were evaluated using the RB model, using an approach similar to arsenic expressions developed using expressions similar to equations 5, 7 and 16. The calculated data for bismuthate capacities and distribution ratios are shown in Fig 5 and 6 respectively. The equilibrium constants for impurities reactions are presented in Table 2. The Gibbs Energy for the $M_{3/2}BiO_4$ (M= Mg, Cu) compounds are not available in the literature. Hence, the bismuthate capacity was calculated for a hypothetical $FeO\text{-}FeO_{1.5}\text{-}SiO_2$ slag. The equilibrium constant (K_{Fe}) for the $Fe_{3/2}BiO_4$ formation reaction was used from the Table 2. Because an absence of data the quantities of MgO and $CuO_{0.5}$ in equations 5, 7 and 16 were excluded from the slag composition at 1573 K and pSO_2 of 0.1 atm. The available experimental pO_2 and $\{n_T\}$, data of γ_{Bi} in the Cu matte and the a_{FeO} in the $FeO\text{-}FeO_{1.5}\text{-}SiO_2$ system were used in these calculations.

For the $FeO\text{-}FeO_{1.5}\text{-}SiO_2$ slags at 1573, the calculated RB model log C_{BiO4}^{3-} and L_{Bi} shows that the model data agrees well with the experimental data below the Cu matte grade of 70 wt pct of Cu. But for the RB model data of log C_{BiO4}^{3-} and L_{Bi} above the Cu matte grade of 70 wt pct of Cu are higher than the experimental data. As mentioned above, the data for $M_{3/2}BiO_4$ for M=Cu or Mg was not included in the calculations. The addition of basic oxides such as CaO to iron oxide slags increases the Fe_2O_3 content up to about 20 wt%, (Rosenqvist ,1983), which decreases the capacity of the slag to retain the impurity. The Fe_2O_3, which is known as an acidic component due to its tendency to consume rather than supply oxygen, lowers the a_{FeO} value in slag, resulting in a decrease in the impurity capacity value. Thus, addition of MgO in the calculation of Bismuthate capacities using equations 5, 7 and 16, expected to decrease the bismuthate capacity and also decrease the distribution ratios, by which their calculated data will be closer to the experimental data. Hence, the availability of reliable thermodynamic data for slag components and impurity compounds in slags and in mattes or liquid metals are essential for the accurate prediction of impurity capacities and their distribution ratios. Further studies are in progress in extending the RB model for the prediction of capacities and distribution ratios of other impurities, such as Se and Te in copper and other non-ferrous metal slags.

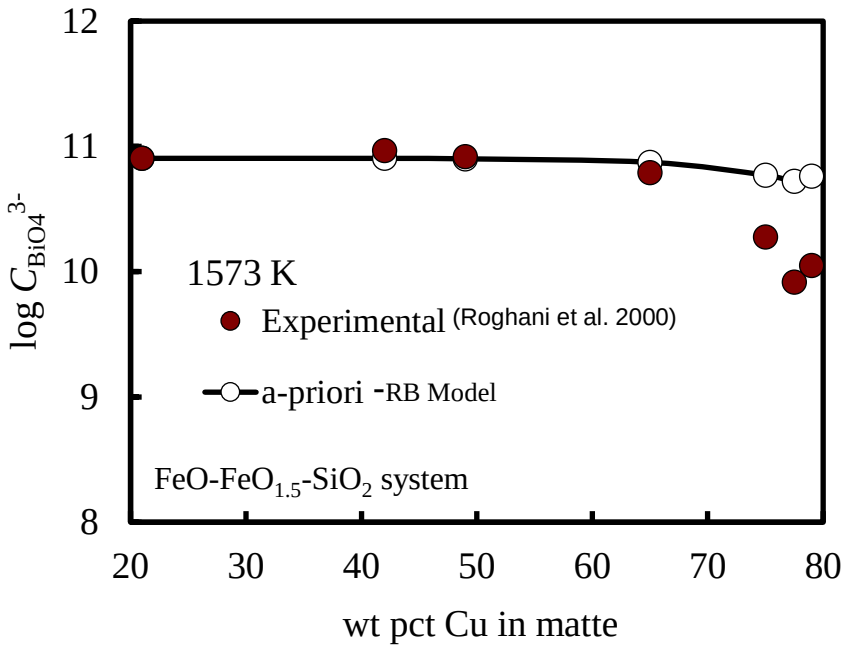

FIG 5-Bismuth capacity of FeO-$FeO_{1.5}$-$CuO_{0.5}$-MgO-SiO_2 slag vs wt pct Cu in matte at 1573 K.

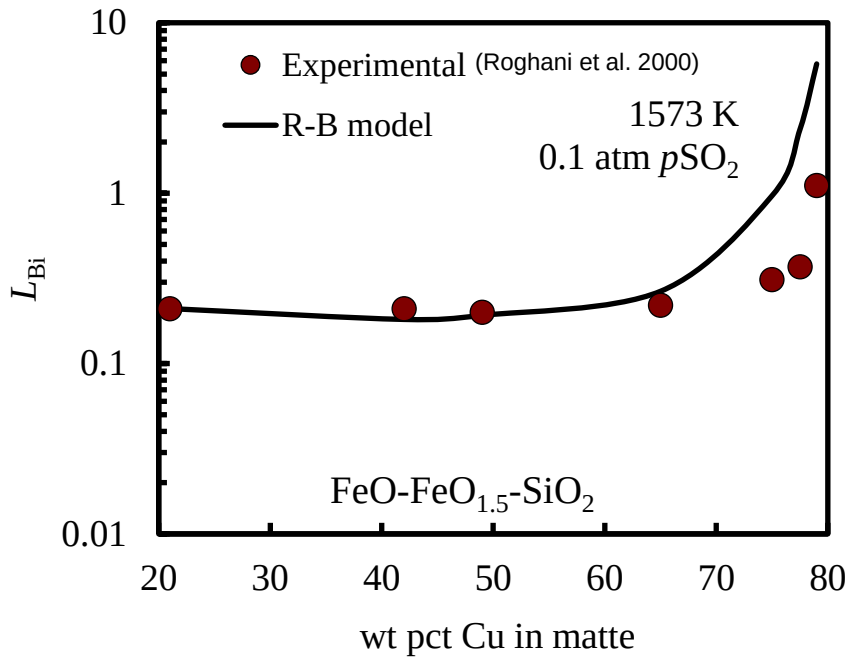

FIG 6- Distribution coefficient of Bismuth of FeO-$FeO_{1.5}$-$CuO_{0.5}$-MgO-SiO_2 slag vs wt pct Cu in matte at 1573 K.

CONCLUSIONS

The impurity (As, Sb and Bi) capacities of iron silicate slags in equilibrium with copper mattes at 1573 K were calculated *a priori* using the RB model. The predicted impurity capacities are in very good agreement with the experimental data. An expression for the relationship between the impurity capacity and the impurity distribution ratio for copper slags and the copper mattes was derived. The derived impurity distribution ratios between the slags and the copper mattes found to be in particularly good agreement with the experimental data for multi-component slags. Such predictions are useful in understanding the behaviour of impurities in the current and eventually future non-

ferrous metal process. The impurity capacities of slags are directly proportional (i) to the equilibrium constant K_M, and (ii) to the values of a_{MO}, which are related to the solution properties. The availability of reliable thermodynamic data for slag components and impurity compounds in slags and in mattes or liquid metals are essential for the accurate prediction of impurity capacities and their distribution ratios.

The RB model is an invaluable tool for the optimization of impurity removal in the existing processes and for the development of new processes. The *a-priori* prediction of other impurity capacities such as Se and Te in non-ferrous metal smelting slags and mattes using RB model is possible and such predictions are very useful in understanding the behavior of impurities in the current and eventually future non-ferrous metals technologies.

ACKNOWLEDGEMENTS

The author acknowledges the financial support from the National Science Foundation (NSF) and ACIPCO for this research project. Author also thanks the Department of Metallurgical and Materials Engineering, The University of Alabama for providing the experimental and analytical facilities.

REFERENCES

Bale, C. W., A. D. Pelton, and W. T. Thompson (2002). FactSage 5.1: Thermochemical Software for Windows.TM Montreal, Quebec: Thermfact Ltd.

Chen, B., Reddy, R.G., and Blander, M.,(1989), Sulfide capacities of CaO-FeO-SiO2 Slags, *3rd International Conference on Molten Slags and Fluxes*, Glasgow, Scotland, pp. 270-272.

Derin, B. and Ramana G. Reddy (2003). Sulfur and Oxygen Partial Pressure Ratios Prediction in Copper Flash Smelting Plants Using Reddy-Blander Model, TMS, PA, USA, Vol. 1, pp. 625-632.

Derin, B., O. Yucel and R. G. Reddy (2005). Sulfide Capacities of $PbO-SiO_2$ and $PbO-SiO_2-AlO_{1.5}$ (sat.) Slags, Mining and Materials Processing Institute of Japan (MMIJ), Kyoto, Japan, 1279-1287.

Derin, B., O. Yucel and R. G. Reddy (2006). Predicting of Sulfide Capacities of Industrial Lead Smelting Slags, Advanced Processing of Metals and Materials, TMS, PA, USA, Vol. 1, 237-244.

Derin, B., O. Yucel and R. G. Reddy (2011). Sulfide Capacity Modelling of $FeOx-MO-SiO_2$ (MO=CaO, MnO, MgO) Melts, Minerals & Metallurgical Processing, Vol. 28 (1), 33-36.

Derin, B., Onuralp Yucel and Ramana G. Reddy (2004). Modelling of Sulfide Capacities of Binary Titanate Slags, EPD Congress 2004, TMS, PA, USA, 155-160.

Flood, H., and Grjotheim, K., (1952), Thermodynamic calculation of slag equilibria, *Journal of the Iron and Steel Institute*, Vol. 171, pp. 64-70.

Font, J. M. and R. G. Reddy (2003), Modeling of Impurity Distribution between Mattes and Slags, Copper 2003, Vol. IV, Chile, pp. 301-313.

Font, J. M. and R. G. Reddy (2005). Modelling of Antimonate Capacity in copper and Nickel Smelting Slags, Trans. Inst. Min. Metall. C, Vol. 114, C160-C164.

Font, J. M., M. Hino and K. Itagaki (1998): Minor Elements Distribution between Iron-Silicate Base Slag and Ni_3S_2-FeS Matte under High Partial Pressures of SO_2, Mat. Trans. JIM, vol. 39, 1998, 834-840

Font, J. M., M. Hino and K. Itagaki (1998a): Thermodynamic Evaluation of Distribution Behaviour of VA Elements in Nickel Matte Smelting, Met. Rev. of MMIJ, vol. 15-2, 202-220

Font, J. M., M. Hino and K. Itagaki (1999): Phase Equilibrium Minor and Elements Distribution between Iron-Silicate Base Slag and Nickel-Copper-Iron Matte at 1573 K under High Partial Pressures of SO_2, Mat. Trans. JIM, vol. 40, 20-26

Font, J. M., M. Hino and K. Itagaki (2000): Phase Equilibrium and Minor-Element Distribution between Ni_3S_2-FeS Matte and Calcium Ferrite slag under High Partial Pressures of SO_2, Metall. Trans. B, vol. 31B, 1231-1239

I.V. Kojo, P. A. Taskinen and K. R. Lilius, The Thermodynamics of copper fire refining by Sodium Carbonate, Second international Symposium on Metallurgical Slags and Fluxes, TMS, Warrendale, USA, pp. 723-737, 1984.

Larouche, P., (2001), Minor Elements in Copper Smelting and Electrorefining, M.S. Thesis, Mining and Metallurgical Engineering, McGill University, Montreal, Canada, 165 pp.

Nikolov, S., H. Jalkanen and M. Kyto (1992), Distribution of some impurity elements between high grade copper matte and calcium ferrite slag, 4th Inter. Conf. on Molten Slags and Fluxes, Sendai, ISIJ, 560-565

Pelton, A. D., (1999). Thermodynamic Calculation of gas solubilities in oxide melts and glasses, Glastechnische berichte, Vol. 72, 40-62.

Pelton, A. D., (2000). Thermodynamic Modelling of Complex Solutions, The Brimacombe Memorial Symposium, ISS, CIM, TMS, PA, USA, 763-780.

Pelton, A.D. G. Eriksson and A. Romero-Serrano (1993): Calculation of sulfide capacities of multi-component slags, Metall. Trans. B, Vol. 24B, 817-825

Reddy, R. G. (2003). Emerging Technologies in Extraction and Processing of Metals, Metallurgical and Materials Transactions B, Vol. 34B, 137-152.

Reddy, R. G. and J. M. Font (2003). Arsenic Capacities of Copper Smelting Slags, Metallurgical and Materials Transactions B, Vol 34B, 565-571.

Reddy, R. G., and M. Blander (1987). Modeling of sulfide capacities of silicate melts, Metallurgical Transactions 18B, 591-596.

Reddy, R. G., and M. Blander (1989). Sulfide capacities of MnO-SiO2 slags, Metallurgical Transactions 20B, 137-140.

Reddy, R. G., and W. Zhao (1995). Sulfide capacities of Na2O-SiO2 melts, Metallurgical and Materials Transactions 26B, 925-928.
Reddy, R. G., H. Hu, and M. Blander (1992). Sulfide capacities of silicate slags, Proceedings of the Fourth International Conference on Molten Slags and Fluxes, 144-148.
Reddy, R.G., (2003a), Impurity Capacities in Metallurgical Slags, *Yazawa International Symposium, Materials Processing Fundamentals and New Technologies*, TMS, Vol. 1, pp. 25-48.
Roghani, G, M. Hino and K. Itagaki (1997): Phase Equilibrium and Minor Elements Distribution between SiO_2-CaO-FeO_X-MgO Slag and Copper Matte at 1573 K under High Partial Pressures of SO_2, Mater. Trans. Jpn. Inst. Met., JIM, vol. 38, 707-713
Roghani, G, Y. Takeda and K. Itagaki (2000): Phase Equilibrium and Minor Element Distribution between FeO_X-SiO_2-MgO-Based Slag and Cu_2S-FeS Matte at 1573 K under High Partial Pressures of SO_2, Metall. Trans. B, vol. 31B, pp. 705-712
Roine, A, (2022) HSC Chemistry software, ver. 7.1, Outokumpu Research Oy, Pori, Finland
Rosenqvist, T (1983): Proceeding for the Advances in Sulfides Smelting Symposium, TMS-AIME, Vol. 1, 239-255
Yahya, A. and Ramana G. Reddy (2011). Sulfide Capacities of CaO-MgO-$AlO_{1.5}$, MgO-MnO- $AlO_{1.5}$ and CaO-MgO-MnO-$AlO_{1.5}$ Slags, Trans. Inst. Min. Metall. C, Vol. 120 (1), 45-48.